ELSEVIER

International Journal of Mass Spectrometry 223–224 (2003) 159–168

International Journal of Mass Spectrometry

www.elsevier.com/locate/ijms

Gas-phase complexes: noncovalent interactions and stereospecificity

D. Scuderi[a,b], A. Paladini[a], M. Satta[a], D. Catone[a], A. Filippi[b], S. Piccirillo[c], A. Laganà[a], M. Speranza[b], A. Giardini Guidoni[a,d,*]

[a] *Dipartimento di Chimica, Università di Roma "La Sapienza", pl. A. Moro 5, I-00185 Rome, Italy*
[b] *Facoltà di Farmacia, Dipartimento di Studi di Chimica e Tecnologia delle Sostanze Biologicamente Attive, Università di Roma "La Sapienza", pl. A. Moro 5, I-00185 Rome, Italy*
[c] *Università di Roma "Tor Vergata" Dipartimento di Scienze e Tecnologie Chimiche, Via della Ricerca Scientifica, I-00133 Rome, Italy*
[d] *CNR-IMIP (sezione Istituto Materiali Speciali), I-85050 Tito Scalo (Pz), Italy*

Received 15 January 2002; accepted 20 March 2002

Dedicated to Professor Werner Lindinger a good friend and an outstanding chemist.

Abstract

Chiral recognition is a fundamental phenomenon in life sciences based on the enantioselective complexation of a chiral molecule with a chiral selector. The diastereomeric aggregates, formed by complexation, are held together by a different combination of intermolecular forces and are, therefore, endowed with different stability and reactivity. Determination of these forces, which are normally affected in the condensed phase by solvent and supramolecular interactions, requires the generation of the diastereomeric complexes in an isolated state and their kinetic and spectroscopic investigation. This paper concerns enantiodiscrimination of chiral molecules in the gas phase through the application of various ESI-MS^n-CID and REMPI-TOF methodologies. The measurement of the fragmentation thresholds of diastereomeric clusters by these techniques allowed to shed light upon the nature and the magnitude of the intrinsic interactions which control their formation and which affect their stability and reactivity. (Int J Mass Spectrom 223–224 (2003) 159–168)

Keywords: Gas-phase enantioselectivity; Aminophosphonic acids; Metal clusters; Chirality; Mass spectrometry

1. Introduction

Molecular clusters play a key role in the molecular scale explanations of macroscopic phenomena, being in a state which is in between the condensed and isolated gas phase. In this state, the lack of interactions with the external environment facilitates the precise determination of the intermolecular forces involved in molecular aggregation and their extension to the macroscopic scale. The existence, the structure, the stability, the physicochemical properties, and the evolution dynamics of a molecular aggregate depend upon a sensitive balance between attractive and repulsive noncovalent interactions. This balance may produce the unique feature of a structure-dependent affinity towards only one enantiomer of a chiral molecule. Few research topics, such as chiral recognition have surpassed the purely chemical threshold, interlocking the physical and life sciences, and attracting the interest of the scientists [1]. In chemistry,

* Corresponding author. E-mail: anna.giardini@uniromal.it

1387-3806/02/$ – see front matter
PII S1387-3806(02)00787-X

specific chirality effects in diastereomeric ground and transition structures are at the origin of many enantioselective syntheses [2]. In biochemistry, the same effects control the highly enantioselective binding of a target substrate to proteins in the chiral cavity of enzymes, antibodies, or sensorial receptors [3].

Molecular-scale investigation of isolated clusters was allowed by the development of gas-phase methodologies as laser spectroscopy and mass spectrometry, but only recently these methodologies have been applied to the study of chiral systems [4,5]. In particular, electrospray ionization mass spectrometry (ESI-MS) [6–8] and resonance-enhanced multi-photon ionization [5,9] coupled with time-of-flight (REMPI-TOF) mass spectrometry, proved most useful for this purpose. Both techniques rely on the measure of the different stability of diastereomeric complexes arising from the combination of a chiral molecule with an enantiomeric selector.

This paper is aimed at reporting results of a comprehensive study on the enantiodiscrimination of chiral molecules in the gas phase through the application of ESI-MS^n collision-induced dissociation (CID) and REMPI-TOF methodologies. The mass-resolved R2PI spectra of diastereomeric clusters of (*R*)-(+)-1-phenyl-1-propanol ($\mathbf{P_R}$), (*R*)-(+)-1-phenyl-1-ethanol ($\mathbf{E_R}$), and (*R*)-(−)-1-indanol ($\mathbf{I_R}$) with water and (*R*)-(−)- and (*S*)-(+)-2-butanol ($\mathbf{B_R}$ and $\mathbf{B_S}$), (*R*)-(−)- and (*S*)-(+)-2-butylamine ($\mathbf{A_R}$ and $\mathbf{A_S}$), and (*R*)-(−)- and (*S*)-(+)-2-hexanol ($\mathbf{X_R}$ and $\mathbf{X_S}$) are discussed. The ESI-MS^n-CID measurements concern trimeric clusters ions $[\mathbf{M}\cdot(\boldsymbol{ref})_2\cdot\mathbf{S}]^+$ between first-group metal ions (M^+) and chiral α-aminophosphonic acids (***ref*** and **S**). The α-aminophosphonic acids investigated are (*R*)-(−)- and (*S*)-(+)-(1-aminoethyl) phosphonic acid ($\mathbf{ame_R}$ and $\mathbf{ame_S}$), (1*R*)-(+)- and (1*S*)-(−)-(1-amino-2-methylpropyl) phosphonic acid ($\mathbf{amp_R}$ and $\mathbf{amp_S}$).

2. Experimental methodologies

2.1. REMPI-TOF

The experimental set-up, which combines a supersonic molecular beam, two Nd-YAG pumped dye lasers and a TOF mass spectrometer, has been elsewhere described [10,11]. Supersonic beam production of the adducts is obtained by adiabatic expansion of a carrier gas (Ar) seeded with a selected chromophore (**C**) and solvent molecule (***solv***) through a heatable pulsed nozzle of 400-μm i.d. The concentration is maintained enough low to minimize the production of heavier clusters. The skimmed supersonic jet (1-mm skimmer diameter) enters into a second chamber equipped with a TOF mass spectrometer. Molecules and clusters in the beam are excited and ionized by one or two tunable dye lasers and the ionized species are detected by a channeltron. The mass-selected photoionization signals are recorded and averaged by a digital oscilloscope and stored on a PC.

One color R2PI experiments (1cR2PI) involve electronic excitation of the species of interest by absorption of one photon $h\nu_1$ and ionization by absorbing a second photon $h\nu_1$. Mass discrimination of the ionized complex may be complicated by fragmentation processes, due to the excess energy gained during ionization.

The ionization and fragmentation thresholds have been obtained by the photoionization efficiency curves through a two color R2PI (2cR2PI) sequence: (i) the first exciting laser ($h\nu_1$) is tuned on the $S_1 \leftarrow S_0$ transition of the species of interest; (ii) the laser intensity is lowered to about 1% of the initial fluence to minimize the $h\nu_1$ absorption; (iii) a second laser ($h\nu_2$) is scanned through the cluster ionization and fragmentation threshold regions. The photoionization spectra were corrected for the effect of the electric field strength (200 V/cm) produced by the extraction plates of the TOF spectrometer.

The binding energy D_0'' of the **C**-***solv*** adduct is computed from the difference between its dissociative ionization threshold $AE[\mathbf{C}]^+ = h\nu_1[\mathbf{C}\text{-}sol\boldsymbol{v}]^* + h\nu_2[(\mathbf{C})^+ + sol\boldsymbol{v}]$ and the ionization threshold of the bare **C**, i.e., $IP[\mathbf{C}] = h\nu_1[\mathbf{C}]^* + h\nu_2[\mathbf{C}]^+$. The dissociation energy $D_0{}^+$of the ionic cluster $[\mathbf{C}\text{-}sol\boldsymbol{v}]^+$ is calculated from the difference between its dissociative ionization threshold, $AE[\mathbf{C}]^+ = h\nu_1[\mathbf{C}\text{-}sol\boldsymbol{v}]^* + h\nu_2[(\mathbf{C})^+ + sol\boldsymbol{v}]$, and its ionization threshold $IP[\mathbf{C}\text{-}sol\boldsymbol{v}] = h\nu_1[\mathbf{C}\text{-}sol\boldsymbol{v}]^* + h\nu_2[\mathbf{C}\text{-}sol\boldsymbol{v}]^+$.

2.2. ESI-MS^n

The CID experiments have been performed by using both a commercial API 100/300 triple-quadrupole (QqQ) mass spectrometer from Perkin Elmer Sciex, equipped with an ESI source and a syringe pump [12]. Operating conditions for the ESI source have been as follows: spray voltage, 3.8 kV; capillary temperature, 298 K; sheath gas (N_2) flow rate, 30 units (roughly 0.75 L/min). The selected gas phase complexes have been generated by electrospraying at a flow rate of 10 μL/min water:methanol (50:50) solutions containing equimolar amounts (10 μM each) of the optically pure solvent molecule and a chiral reference compound. The CID experiments on the so-formed diastereomeric complexes have been conducted in the positive ion mode. In the full scan QqQ-MS^2 mode, the diastereomeric cluster ions have been isolated in the first mass analyzing quadrupole Q, excited in the second "rf-only" quadrupole *q* by collision with N_2 (pressure ca.10 mbar; energy range 6–12 eV in the laboratory frame), and eventually analyzed in the third quadrupole Q of the instrument.

3. Computational methods

Electronic ground state structure and vibrational frequencies of the $\mathbf{P_R}$, $\mathbf{E_R}$, and $\mathbf{I_R}$ molecules have been computed by density functional calculations based on Becke's three parameter hybrid functional added by the LYP correlation functional (B3LYP). The 6-31G** Gaussian split valence basis set, in which *p* functions are added to H atom and *d* functions to heavy atoms, has been used [13].

A set of cluster geometries has been generated by binding a water molecule (either as proton acceptor or donor) to the $\mathbf{P_R}$, $\mathbf{E_R}$, and $\mathbf{I_R}$ molecules. These structures have been then optimized using the semi-empirical PM3 Hamiltonian, in order to obtain input cluster geometries for the full ab initio optimization conducted at the B3LYP/6-31G** level of theory. The vibrational frequency analysis has been performed at the above theoretical level to obtain the zero-point energy (ZPE) for each optimized molecular monomer and cluster structures.

Calculated intermolecular D_0'' energies have been corrected by using the counterpoise method in order to avoid the basis set superposition error (BSSE) [14]: the B3LYP/6-31G** optimized cluster geometries have been used to compute the energies of the monomers alone and in the presence of the partner ghost basis sets. All the ab initio calculations have been performed using the Gaussian 98 package [15].

Some insights into the intermolecular forces operating in the diastereomeric, $[\mathbf{M}\cdot(\boldsymbol{ref})_2\cdot\mathbf{S_S}]^+$ and $[\mathbf{Me}\cdot(\boldsymbol{ref})_2\cdot\mathbf{S_R}]^+$, complexes can be obtained from the analysis of their structures and binding energies as calculated at the Molecular Mechanics MM2 Force Field level of theory [16], in which the electrostatic energy contribution was calculated by bond–dipole interactions. Geometry optimization has been obtained by using the Polak–Ribier (conjugate-gradient) algorithm with a 0.4 kJ/mol RMS gradient threshold.

4. Results and discussion

4.1. R2PI spectroscopy of hydrated clusters

Hydrated aromatic molecules are simple models to study the selectivity and the function of biologically active systems. The role of hydrogen-bond interaction and molecular conformation has been studied for many aromatic molecule—water clusters, including molecules of biological interest [17–19]. In this section, 1cR2PI spectra of hydrated adducts of benzylic alcohol derivatives $\mathbf{E_R}$, $\mathbf{P_R}$, and $\mathbf{I_R}$ are reported and discussed. The measure of the shifts and the binding energies of these systems can provide some information on the effects of water, which can acts both as proton donor and acceptor in many organic and biological compounds.

The 1cR2PI spectra of the hydrated adducts of $\mathbf{E_R}$, $\mathbf{P_R}$, and $\mathbf{I_R}$ are reported in Fig. 1. Several conformers may be generated in the beam and their vibronic transitions generally complicate the mass-resolved 1cR2PI excitation spectra. This problem is less evident in

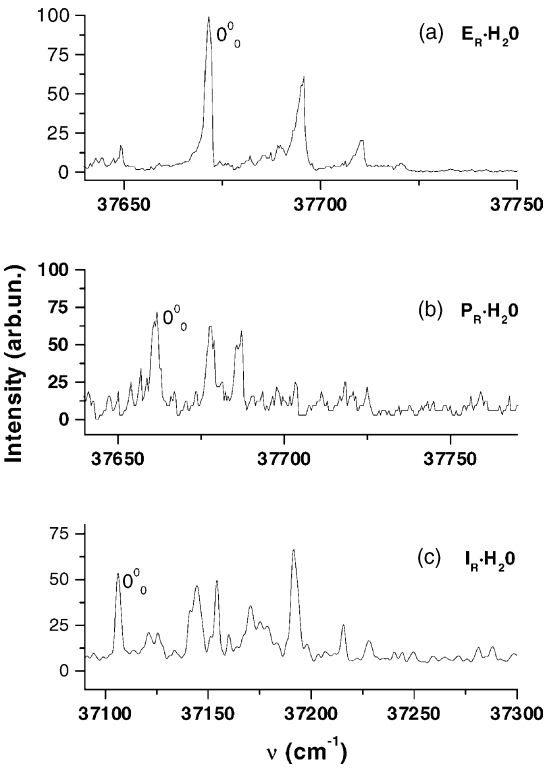

Fig. 1. Mass-resolved 1cR2PI excitation spectrum of $\mathbf{E_R \cdot H_2O}$ (a), $\mathbf{P_R \cdot H_2O}$ (b), and $\mathbf{I_R \cdot H_2O}$ (c) clusters measured at a total stagnation pressure of 4×10^5 Pa. The $0_0{}^0$ electronic origin of the $S_0 \leftarrow S_1$ transition of the bare chromophores are respectively 37,618, 37,618, and 37,067 cm^{-1} and those of the clusters are marked in the figure.

the $\mathbf{E_R \cdot H_2O}$ cluster (Fig. 1a), as demonstrated by its comparatively simple spectrum [20,21]. With $\mathbf{C = P_R}$ (Fig. 1b) or $\mathbf{I_R}$ (Fig. 1c), different stable conformations are predicted and found either in the isolated molecule and in its hydrated cluster [22]. A blue shift of the electronic transition of each of the three hydrated clusters with respect to the $0_0{}^0$ $S_1 \leftarrow S_0$ band origin of the bare chromophore is observed. This indicates that the energy gap between the S_0 and S_1 state increases by monohydration. A blue shift of the electronic transition in many 1:1 aromatic molecule:water cluster is not unusual and can be related to an O–H $\cdots$ π interaction between the aromatic ring of chromophore and the water molecule [18,19,23]. This conclusion is corroborated by the B3LYP/6-31G** optimized geometries of the most stable $\mathbf{C \cdot H_2O}$ ($\mathbf{C = E_R}$, $\mathbf{P_R}$, or $\mathbf{I_R}$) conformers (Fig. 2a–c, respectively), which are characterized by water acting as proton acceptor for the benzylic proton of **C** as well as proton donor towards the aromatic ring of the chromophore. A fair agreement is also observed between the B3LYP/6-31G** computed binding energies of $\mathbf{C \cdot H_2O}$ ($\mathbf{C = E_R}$ or $\mathbf{P_R}$) and the experimental 2cR2PI values [20–22]. In this connection, it should be taken into account that poor Frank–Condon factors for the vertical transition from the S_1 excited state to the ionic state [24] lead to an overestimation of ionization energy of the molecule, and consequently the phenomenological binding energy of the cluster is a lower limit of the actual value. An overestimation of the computed binding energy due to an excess of BSSE correction [22,25], cannot be excluded.

4.2. R2PI enantiodifferentiation of chiral molecules

Enantiodifferentiation of neutral chiral molecules in the gas phase can be obtained by mass-resolved R2PI spectroscopy of their adducts with chiral partners. Diastereomeric pairs are characterized by the nonequivalence of their interaction energy in both the ground and excited states and, therefore, they exhibit different spectroscopic properties [5,9]. Fig. 3 shows the R2PI excitation spectra of the diastereomeric complexes of $\mathbf{E_R}$ with $\mathbf{B_R}$ and $\mathbf{B_S}$ (Fig. 3a), $\mathbf{P_R}$ with $\mathbf{A_R}$ and $\mathbf{A_S}$ (Fig. 3b), and $\mathbf{I_R}$ with $\mathbf{X_R}$ and $\mathbf{X_S}$ (Fig. 3c). The spectra are complicated by the vibronic transitions associated to the conformers of the adducts. As already observed for other chiral clusters [20,26], the examined complexes display a spectral signature characterized by a significant red shift $\Delta\nu$ of the $0_0{}^0$ $S_1 \leftarrow S_0$ transition relative to that of the bare chromophore. These spectral shifts reflect the combined effect of the electrostatic and dispersive interactions between **C** and ***solv*** on the HOMO and LUMO energies of the chromophore. The homo chiral clusters, e.g., $\mathbf{E_R \cdot B_R}$, exhibits a red shift ($\Delta\nu_{\text{homo}}$) less negative than that displayed by the hetero chiral analog, i.e., $\mathbf{E_R \cdot B_S}$, ($\Delta\nu_{\text{hetero}}$). Their differences, $\Delta\Delta\nu = \Delta\nu_{\text{homo}} - \Delta\nu_{\text{hetero}} = +12\,\text{cm}^{-1}$ ($\mathbf{E_R \cdot B_R/B_S}$), $+18\,\text{cm}^{-1}$ ($\mathbf{P_R \cdot A_R/A_S}$), and $+30\,\text{cm}^{-1}$

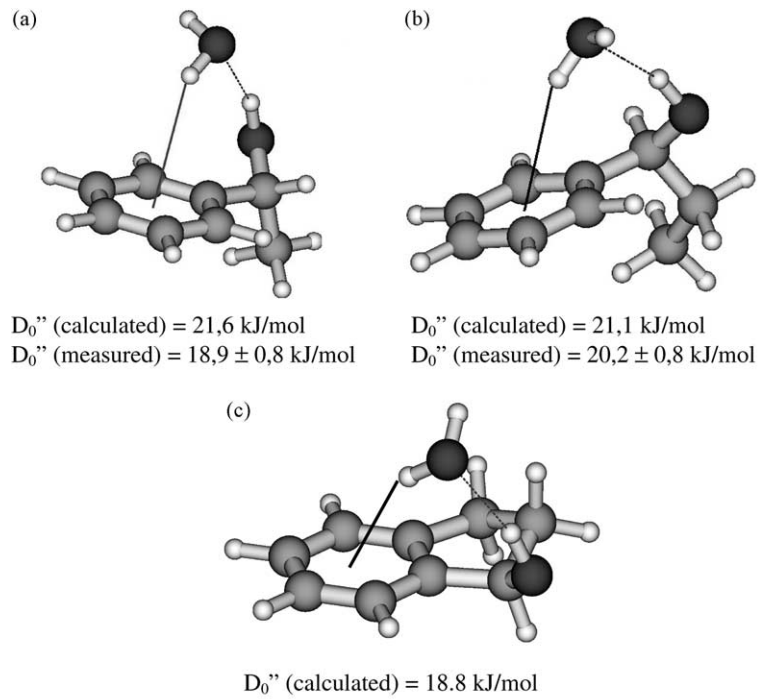

Fig. 2. Calculated minimum energy structures of $\mathbf{E_R}\cdot\mathbf{H_2O}$ (a), $\mathbf{P_R}\cdot\mathbf{H_2O}$ (b), and $\mathbf{I_R}\cdot\mathbf{H_2O}$ (c). Predicted and measured binding energies are also reported.

($\mathbf{I_R}\cdot\mathbf{X_R}/\mathbf{X_S}$), are consistent with an $S_1 \leftarrow S_0$ energy gap of the hetero chiral complex which is smaller than that of the corresponding homo chiral adduct. Similar $\Delta\Delta\nu$ values were determined for other diastereomeric pairs [21,27].

The 1cR2PI mass fragmentation pattern of the selected diastereomeric clusters gives some insight on the steric effects observed in the excitation spectra. In 1cR2PI experiments, an excess vibrational energy is imparted to the ionic adduct which undergoes extensive fragmentation. The spectral patterns of the fragment ions are found to be the same of that of the parent ion [27]. Ionization of the homo and hetero complexes of $\mathbf{E_R}$, $\mathbf{P_R}$, and $\mathbf{I_R}$ with various chiral alcohols gives rise to the same fragment distribution, characterized by the loss of solvent, alkyl radical, or water. When $\boldsymbol{solv}$ is $\mathbf{A_R}/\mathbf{A_S}$, ionization of the complexes leads also to the formation of a $\boldsymbol{solv}\cdot H^+$ fragment due to proton transferred from the ionized chromophore to the amines [27,28]. The occurrence of this intracomplex process, which is completely absent when $\boldsymbol{solv}$ = aliphatic alcohol, is favored by the high proton affinity of the selected amines. Table 1 shows the relative ion abundances of $\mathbf{I_R}$ clusters with $\mathbf{B_R}$ and $\mathbf{B_S}$, $\mathbf{X_R}$ and $\mathbf{X_S}$, and $\mathbf{A_R}$ and $\mathbf{A_S}$, taken at the frequencies of the electronic origins of the corresponding clusters. The differences in the relative ion abundances arising from fragmentation of each diastereomeric pair are reproducible and are large enough to allow chiral discrimination [5,27]. It can be seen that when $\boldsymbol{solv}$ is $\mathbf{A_R}/\mathbf{A_S}$, a more extensive fragmentation is observed in the homo chiral adducts while a reversed fragmentation trend is observed when $\boldsymbol{solv}$ is $\mathbf{B_R}/\mathbf{B_S}$ or $\mathbf{X_R}/\mathbf{X_S}$ [28,29]. These data parallel to those found when $\mathbf{C}$ = $\mathbf{E_R}$ or $\mathbf{P_R}$ [27,28]. The measured binding energies of these chromophores with $\mathbf{B_R}/\mathbf{B_S}$ [9,20,26] indicate that the hetero chiral clusters are less bounded than the homo chiral ones. This is probably the reason why

a larger fragmentation extent is observed by 1cR2PI process for hetero clusters $\mathbf{E_R}\cdot\mathbf{B_S}$ and $\mathbf{P_R}\cdot\mathbf{B_S}$ with respect to the corresponding homo diastereomers.

The $\Delta\Delta\nu$ values and the highly reproducible differences in the R2PI fragmentation pattern of diastereomeric clusters represent useful tools for enantiodiscrimination of the chiral molecules in the gas phase and provide some insights into the balance between attractive and steric repulsive forces operating in these systems [5,27,28].

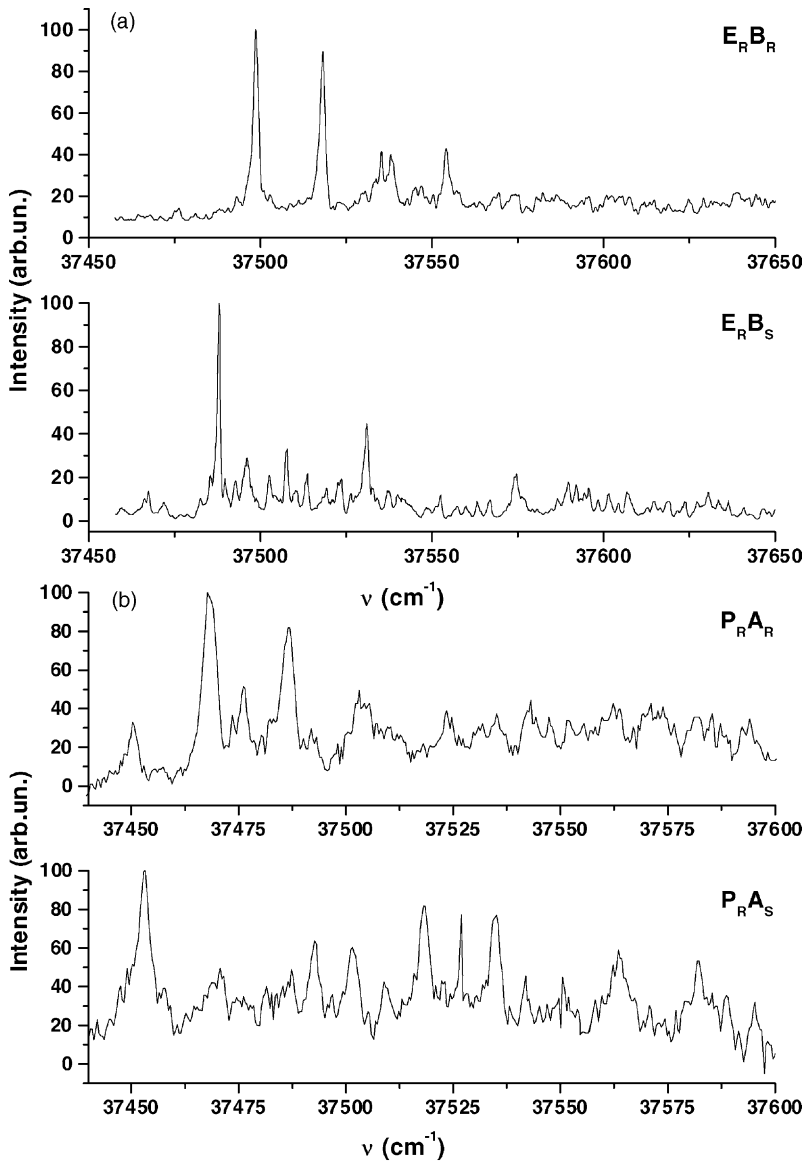

Fig. 3. 1cR2PI excitation spectra of the complexes of (a) $\mathbf{E_R}$ with $\mathbf{B_R}$ and $\mathbf{B_S}$, (b) $\mathbf{P_R}$ with $\mathbf{A_R}$ and $\mathbf{A_S}$, and (c) $\mathbf{I_R}$ with $\mathbf{X_R}$ and $\mathbf{X_S}$ measured at a total stagnation pressure of 4×10^5 Pa. The $0_0{}^0$ electronic origin of the $S_0 \leftarrow S_1$ transition of the bare chromophores are respectively 37,618, 37,618, and 37,067 cm^{-1}, and the shifts are respectively: $\Delta\nu_{\text{homo}} = -119\,\text{cm}^{-1}$ and $\Delta\nu_{\text{hetero}} = -131\,\text{cm}^{-1}$ (a), $\Delta\nu_{\text{homo}} = -109\,\text{cm}^{-1}$ and $\Delta\nu_{\text{hetero}} = -127\,\text{cm}^{-1}$ (b), $\Delta\nu_{\text{homo}} = -134\,\text{cm}^{-1}$ and $\Delta\nu_{\text{hetero}} = -164\,\text{cm}^{-1}$ (c).

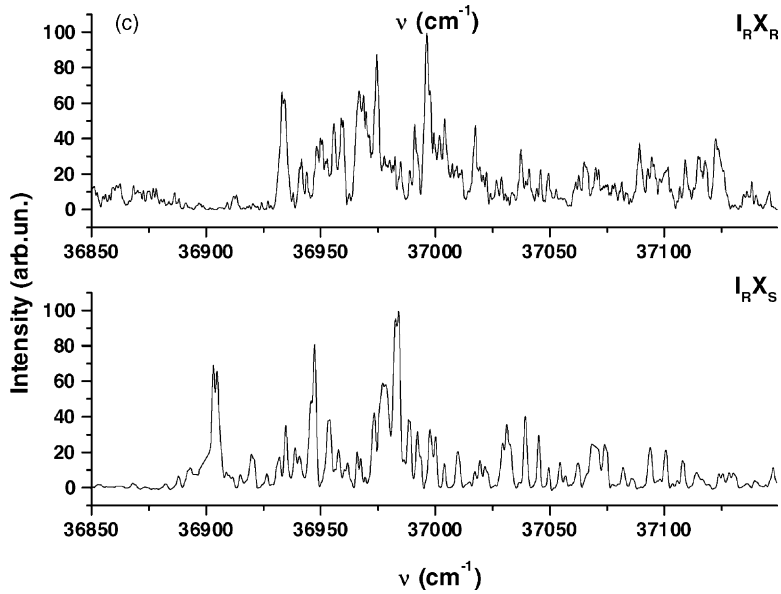

Fig. 3. (*Continued*).

4.3. ESI-MS^2-CID enantiodifferentiation of chiral α-aminophosphonic acids

This section deals with the application of the ESI-MS^2-CID technique to the enantiodiscrimination of several chiral α-aminophosphonic acids. α-Aminophosphonic acids are the analogs of natural α-aminocarboxylic acids present in biological systems. The biological activity of these chiral compounds is governed by the stability of their desolved inclusion complexes into the chiral cavity of an enzyme and, specifically, with its metal ion centers. For this reason, we deemed it important to investigate the affinity of α-aminophosphonic acids towards first-group metals in gaseous phase and how this can be affected by the ligands configuration. The results are discussed in the light of structure calculation performed by using an empirical force field.

According to the foundations of Cooks' kinetic method [6], gas-phase discrimination of chiral solvent $\mathbf{S_R}$ and $\mathbf{S_S}$ is obtained by measuring the relative stability of their diastereomeric complexes with a chiral reference selector ***ref***. CID of the diastereomeric cluster ions $[\mathbf{M}\cdot(\boldsymbol{ref})_2\cdot\mathbf{S_R}]^+$ and $[\mathbf{M}\cdot(\boldsymbol{ref})_2\cdot\mathbf{S_S}]^+$,

Table 1
Relative ion abundances from the R2PI mass spectra of complexes $\mathbf{I_R}\cdot\mathbf{B_R}$ and $\mathbf{I_R}\cdot\mathbf{B_S}$, $\mathbf{I_R}\cdot\mathbf{X_R}$ and $\mathbf{I_R}\cdot\mathbf{X_S}$, and $\mathbf{I_R}\cdot\mathbf{A_R}$ and $\mathbf{I_R}\cdot\mathbf{A_S}$, taken at the corresponding resonant frequencies of each cluster

C	*solv*	Δν	%[C-*solv*]$^+$	%[(C-*solv*)·$\mathbf{H_2O}$]$^+$	%[C]$^+$	% [*solv*·H]$^+$
$\mathbf{I_R}$	$\mathbf{B_R}$	−113	30.6	34.7	34.7	–
	$\mathbf{B_S}$	−127	26.7	24.5	48.8	–
	$\mathbf{X_R}$	−134	49.4	–	50.6	–
	$\mathbf{X_S}$	−164	45.3	–	54.7	–
	$\mathbf{A_R}$	−137	16.6	4.4	53.6	25.4
	$\mathbf{A_S}$	−150	18.4	3.1	42.9	29.5

Spectral shifts (Δν in cm^{-1}) is the difference between the 0_0^0 $S_1 \leftarrow S_0$ electronic transitions of the clusters with respect to that of the bare chromophore.

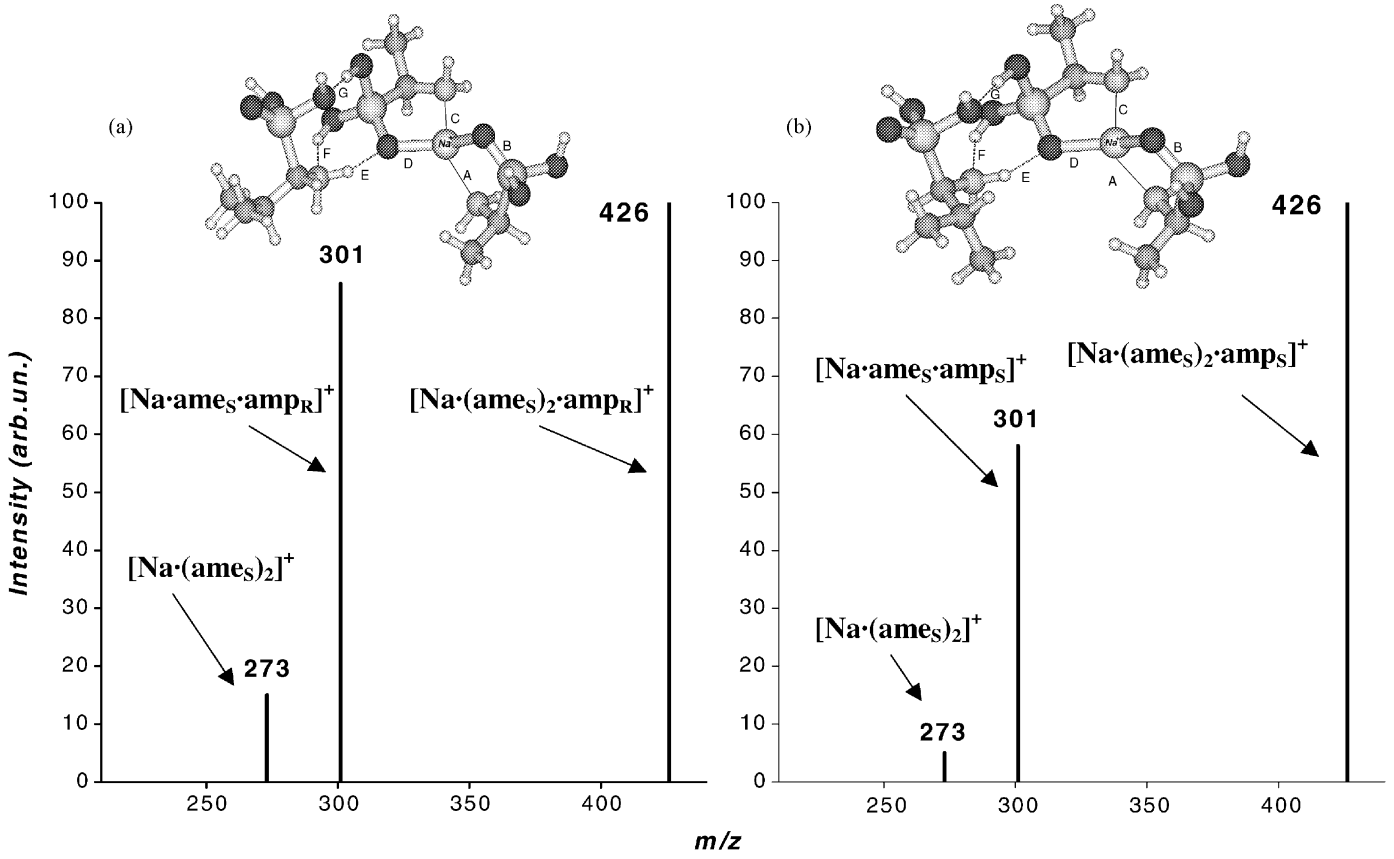

Fig. 4. Typical CID-MS^2 fragmentation spectra of diastereomeric clusters $[\mathbf{Na}\cdot(\mathbf{ame_S})_2\cdot(\mathbf{amp_R})]^+$ (a) and $[\mathbf{Na}\cdot(\mathbf{ame_S})_2\cdot(\mathbf{amp_S})]^+$ (b). The spectra are the result of 300 scans (collision energy 8 eV; lab frame). Calculated minimum energy structures for the clusters $[\mathbf{Na}\cdot(\mathbf{ame_S})_2\cdot(\mathbf{amp_R})]^+$ and $[\mathbf{Na}\cdot(\mathbf{ame_S})_2\cdot(\mathbf{amp_S})]^+$ are also reported.

where $M^+ = H^+$, Li^+, Na^+, and K^+, may produce different fragmentation patterns reflecting the relevant $[\mathbf{M}\cdot\boldsymbol{ref}\cdot\mathbf{S_R}]^+$ and $[\mathbf{M}\cdot\boldsymbol{ref}\cdot\mathbf{S_S}]^+$ vs. $[\mathbf{M}\cdot(\boldsymbol{ref})_2]^+$ stability. It is convenient to define the cluster ions as "homo" when **S** and ***ref*** have the same configuration, and "hetero" in the opposite case. Measurement of the ratio of the "homo" vs. "hetero" ion abundance ratios provides the chiral selectivity R_{chiral}, i.e.:

$$R_{\text{chiral}} = \frac{R_{\text{homo}}}{R_{\text{hetero}}} = \frac{[\mathbf{M}\cdot ref\cdot\mathbf{S_S}]^+/[\mathbf{M}\cdot(ref)_2]^+}{[\mathbf{M}\cdot ref\cdot\mathbf{S_R}]^+/[\mathbf{M}\cdot(ref)_2]^+} \quad (1)$$

if the *S* enantiomer of ***ref*** is employed.

Fig. 4 reports typical CID fragmentation spectra of diastereomeric clusters containing one of the $\mathbf{amp_R}$ and $\mathbf{amp_S}$ enantiomers, as solvent, $\mathbf{ame_S}$ as ***ref***, and a sodium ion ($[\mathbf{Na}\cdot(\mathbf{ame_S})_2\cdot(\mathbf{amp_R})]^+$ and $[\mathbf{Na}\cdot(\mathbf{ame_S})_2\cdot(\mathbf{amp_S})]^+$), together with their calculated structures. Their fragmentation leads essentially to the $[\mathbf{Na}\cdot(\mathbf{ame_S})\cdot(\mathbf{amp_{R,S}})]^+$ and $[\mathbf{Na}\cdot(\mathbf{ame_S})_2]^+$. Analogous results have been found for other metal ion/α-aminophosphonic mixtures investigated [12,29].

The reproducibility of the present method has been investigated changing the chirality of the reference acid ***ref***. The results obtained using the other ***ref*** enantiomer are within ca. 10% error and the uncertainty associated with consecutive measurements of the same system is within 5%.

The average chiral resolution factors R_{chiral} for the diastereomeric clusters investigated are reported in Table 2. An $R_{\text{chiral}} < 1$ value indicates that the hetero chiral complex is more stable than the homo chiral one. For $R_{\text{chiral}} = 1$, there is no stability differences and chiral discrimination is unattainable by this method.[1]

Table 2
Discrimination of the (1-amino-2-methylpropyl) phosphonic acid enantiomers ($\mathbf{amp_S}$ and $\mathbf{amp_R}$) by ESI-MS^2-CID fragmentation of their diastereomeric clusters $[\mathbf{M}\cdot(\boldsymbol{ref})_2\cdot\mathbf{amp_S}]^+$ and $[\mathbf{M}\cdot(\boldsymbol{ref})_2\cdot\mathbf{amp_R}]^+$ ($\mathbf{M}^+ = \mathbf{H}^+$, $\mathbf{Li}^+$, $\mathbf{Na}^+$, and $\mathbf{K}^+$; *ref* = either (*R*)-(−)- or (*S*)-(+)-(1-aminoethyl) phosphonic acid)

$\mathbf{M}^+$	Average R_{chiral}
$\mathbf{H}^+$	0.92 ± 0.04
$\mathbf{Li}^+$	1.14 ± 0.05
$\mathbf{Na}^+$	0.90 ± 0.04
$\mathbf{K}^+$	0.92 ± 0.04

The CID results of Table 2 provide only a stability order for the diastereomeric clusters and indicate that this depends upon the nature of the metal center. Molecular Mechanics MM2 Force Field calculations point to the most probable configuration for $([\mathbf{Na}\cdot(\mathbf{ame_S})_2\cdot(\mathbf{amp})]^+$ as that with the reference molecules $\mathbf{ame_S}$ directly bounded to the metal center and with the analyte placed outside (Fig. 4) [12].

5. Concluding remark

Gas-phase chiral molecules have been enantiodifferentiated after complexation with a chiral selector by using the REMPI-TOF and ESI-MS^n-CID techniques. The wavelength and mass selectivity displayed by gaseous clusters containing chiral and achiral molecules reflect the balance between stereospecific attractive (hydrogen bond, dispersive, charge exchange, etc.) and respulsive (steric) interactions operating in these systems. The spectral shifts observed in the R2PI spectra of clusters attest the role played by $OH\cdots\pi$ interactions in determining their structure. The nature of the forces acting in these complexes has been explored with the support of theoretical calculations.

Acknowledgements

Contract grant sponsor—Ministero della Università e della Ricerca Scientifica e Tecnologica (MURST) and Consiglio Nazionale delle Ricerche (CNR): P.F. MSTAII.

[1] In previous publications (refs. [12,29]), according to Cooks' kinetic method [6], the free-energy difference $\Delta(\Delta G) = \Delta G_{\text{homo}} - \Delta G_{\text{hetero}}$ of diastereomeric $[\mathbf{M}\cdot\boldsymbol{ref}\cdot\mathbf{S}]^+$ was derived from the $\ln R_{\text{chiral}} = \Delta(\Delta G)/RT_{\text{eff}}$ equation, using a T_{eff} value estimated on the grounds of the fragmentation pattern of their $[\mathbf{M}\cdot(\boldsymbol{ref})_2\cdot\mathbf{S}]^+$ precursors. However, a rigorous theoretical analysis of Cooks' method [8] pointed out that the description of the reacting population requires the use of two different temperatures, not determinable at present.

References

[1] H.C. Kolb, M.G. Finn, K.B. Sharpless, Angew. Chem. 40 (2001) 2004.
[2] W.H. Pirkle, T.C. Pochapsky, Chem. Rev. 89 (1989) 327.
[3] D.J. Holme, H. Peck, Analytical Biochemistry, Longman Scientific & Technical Wiely, New York, 1993.
[4] R. Al-Rabaa, E. Bréhéret, F. Lahmani, A. Zehnacker, Chem. Phys. Lett. 237 (1995) 480.
[5] S. Piccirillo, C. Bosman, D. Toja, A. Giardini Guidoni, M. Pierini, A. Troiani, M. Speranza, Angew. Chem. Int. Ed. Engl. 36 (1997) 1729.
[6] (a) W.A. Tao, D. Zhang, E.N. Nikolaev, R.G. Cooks, J. Am. Chem. Soc. 122 (2000) 10598;
(b) W.Y. Shen, P.S.H. Wong, R.G. Cooks, Rapid Commun. Mass Spectrom. 11 (1997) 71.
[7] M. Sawada, Y. Takay, H. Yamada, S. Hirayama, T. Kaneda, T. Tanaka, K. Kamada, T. Mizooku, S. Takeuchi, K. Ueno, K. Hirose, Y. Tobe, K. Naemura, J. Am. Chem. Soc. 117 (1995) 7726, and references therein.
[8] J. Laskin, J.H. Futrell, J. Phys. Chem. A 104 (2000) 8829.
[9] M. Mons, F. Piuzzi, I. Dimicoli, A. Zehnacker, F. Lahmani, Phys. Chem. Chem. Phys. 2 (2000) 5065.
[10] D. Consalvo, A. Van der Avoird, S. Piccirillo, M. Coreno, A. Giardini Guidoni, A. Mele, M. Snels, J. Chem. Phys. 99 (1993) 8398.
[11] A. Latini, D. Toja, S. Piccirillo, A. Giardini Guidoni, S. Piccirillo, M. Speranza, Angew. Chem. Int. Ed. Engl. 38 (1999) 815.
[12] A. Paladini, C. Calcagni, M. Satta, T. Di Palma, M. Speranza, A. Laganà, G. Fago, A. Filippi, A. Giardini-Guidoni, Chirality 13 (2001) 707.
[13] A.D. Becke, J. Chem. Phys. 98 (1993) 5648.
[14] S. Boys, F. Bernardi, Mol. Phys. B 19 (1970) 553.
[15] M.J. Frisch, G.W. Trucks, H.B. Schlegel, G.E. Scuseria, M.A. Robb, J.R. Cheeseman, V.G. Zakrzewski, J.A. Montgomery Jr., et al., Gaussian 98, Revision A.6, Gaussian, Inc., Pittsburgh, PA, 1998.
[16] N.L. Allinger, J. Am. Chem. Soc. 99 (1977) 8127.
[17] B. Brutchy, Chem. Rev. 92 (1992) 1567.
[18] R.J. Graham, R.T. Kroemer, M. Mons, E.G. Robertson, L.C. Snoek, J.P. Simons, J. Phys. Chem. A 103 (1999) 9706.
[19] M. Mons, E. Robertson, J.P. Simons, J. Phys. Chem. A 104 (2000) 420.
[20] A. Giardini Guidoni, S. Piccirillo, D. Scuderi, M. Satta, T.M. Di Palma, M. Speranza, Phys. Chem. Chem. Phys. 2 (2000) 4139.
[21] K. Le Barbu, F. Lahmani, M. Broquier, A. Zehnacker, Phys. Chem. Chem. Phys. 3 (2001) 4684.
[22] M. Satta, A. Latini, S. Piccirillo, T.M. Di Palma, D. Scuderi, M. Speranza, A. Giardini, Chem. Phys. Lett. 316 (2000) 94.
[23] R.N. Pribble, T.S. Zwier, Science 265 (1994) 75.
[24] C.E.H. Dessent, W.D. Geppert, S. Ullrich, K. Muller-Dethlefs, Chem. Phys. Lett. 319 (2000) 375.
[25] A. Courty, M. Mons, I. Dimicoli, F. Piuzzi, M.P. Gaigeot, V. Brenner, P. de Pujo, P. Millie, J. Phys. Chem. 102 (1998) 6590.
[26] A. Latini, M. Satta, A. Giardini Guidoni, S. Piccirillo, M. Speranza, Chemistry 6 (2000) 1042.
[27] A. Giardini-Guidoni, S. Piccirillo, Israel J. Chem. 37 (1997) 439–443.
[28] A. Filippi, A. Giardini, A. Latini, S. Piccirillo, D. Scuderi, M. Speranza, Int. J. Mass Spectrom. 210/211 (2001) 483.
[29] G. Fago, A. Filippi, A. Giardini, A. Laganà, A. Paladini, M. Speranza, Angew. Chem. Int. Ed. Engl. 40 (21) (2001) 4051.